

SEVEN-CELL CAVITY OPTIMIZATION FOR CORNELL'S ENERGY RECOVERY LINAC*

N. Valles[†] and M. Liepe, Cornell University, CLASSE, Ithaca, NY 14853, USA

Abstract

This paper discusses the optimization of superconducting RF cavities to be used in Cornell's Energy Recovery Linac, a next generation light source. We outline the physical constraints in designing these cavities capable of sustaining high beam current (100 mA), with a high bunch repetition rate (1.3 GHz). We discuss the optimization of the seven-cell cavity geometry, both the considerations needed for the center cell design, and results of the end cell design. The optimization aims to: limit the dynamic cryogenic load of the accelerating mode, maintain a low ratio of peak electric to accelerating field to minimize the risk of field emission and maximize higher order mode damping to suppress beam instabilities. We find a design stable under small shape perturbations, and show that a simulated Energy Recovery Linac constructed from these optimized cavities can support average beam currents of 250 mA.

INTRODUCTION

Central to the intended operation of an Energy Recovery Linac (ERL) is the proper design and functioning of the superconducting RF cavities comprising its main accelerating structure. Cornell has chosen to implement superconducting Niobium seven-cell accelerating structures into the main linac design enabling a high current (100 mA), very low emittance (30 pm-rad at 77 pC bunch charge) 5 GeV beam capable of producing short pulses ($\sigma_z/c = 2$ ps) of hard x-rays with a high repetition rate (1.3 GHz) [1]. This paper discusses the physical considerations that must be implemented into the cavity design and the methods used to optimize cavities under these constraints.

The 7-cell cavity is a 1.3 GHz design. This work is an extension of an initial cavity design, by V. Shemelin [2]. This initial cavity design was optimized to obtain a large value of $R/Q \cdot G$ for the fundamental mode (1.3 GHz), and minimizes the dynamic cryogenic load, while limiting the ratio of peak electric to accelerating field E_{pk}/E_{acc} to 2.0, minimizing the risk of electron field emission. These constraints must still be satisfied for any subsequent design.

The ERL must be able to support currents up to its design value of 100 mA. Higher-order mode (HOM) frequency variations, sometimes called frequency spread, between individual cavities unavoidably arise due to small shape variations in the cavities. This frequency spread reduces coherent excitation of dipole modes in the cavity string. Re-

ducing the coherence of dipole modes that can cause instabilities increases the beam current limit in the accelerator. These same shape changes can change the HOM field profile thereby affecting the beam break-up (BBU) parameter, defined as $R/Q \cdot Q_L/f$, where R/Q is the geometry factor of the cavity, Q_L is the loaded Q of the cavity, and f is the frequency of the mode. As the BBU parameter increases, the maximal current through the accelerator is reduced. A good cavity design needs to balance the increase in frequency spread with the decrease in threshold current.

Manufactured cavities obviously deviate slightly from the ideal design. Small shape changes to the cavity are the source of frequency variations, which eliminate coherent effects. The beam break-up parameter is influenced by changes in the field profile. Small shape changes can drastically affect the performance of the cavities.

For this reason, a robust design needs to be stable under manufacturing perturbations, which introduce small shape defects. Currently, machining tolerances for Niobium cavities of $\pm 1/8$ mm have been achieved. Furthermore, standard procedure implements surface preparations such as Buffer Chemical Polishing (BCP) or Electropolishing (EP) of cavities which introduces further variation. Clearly, to achieve a suitable result, the final design should produce cavities that satisfy all the above constraints even under small random shape changes.

METHODS

Starting from a design optimized to minimize cryogenic losses and having $E_{pk}/E_{acc} = 2.0$, the next objective was to find a design that allows the ERL to operate at high beam current. Initially, only the end cells of the cavity were re-optimized to reduce the strength of dipole HOMs. As will be discussed, this design was unstable (with regard to threshold current through the linac) under small shape perturbations, so the center cell shape was also re-optimized to produce a robust cavity design.

Designing a cavity stable under shape perturbations was accomplished by maximizing the frequency width of narrow passbands with strong HOMs. Increasing the width of these passbands effectively increases the coupling between the center cells, making the design more robust.

With the new center cell design, the end cells of the cavity were again optimized. The goal of the optimization is allowing maximal current to pass through the ERL before the beam breaks up due to instabilities. The threshold beam current, I_{th} through the cavity is given by

$$I_{th} = - \frac{2c^2}{e \left(\frac{R}{Q}\right)_\lambda (Q_L)_\lambda \omega_\lambda T_{12}^* \sin(\omega_\lambda t_r)} \quad (1)$$

* Work supported by NSF Award PHY-0131508, the Empire State Development Corporation (ESDC) Energy Recovery Linac Project # U316, and Cornell University.

[†] nrv5@cornell.edu

where ω_λ is the HOM frequency, t_r is the bunch return time, and T_{12} is the 1-2 element of the T matrix [3]. Thus, minimizing the beam break-up parameter, $R/Q \cdot Q_L/f$, increases the beam current through the accelerator. Preliminary studies showed that each BBU parameter should be no greater than $10^5 \Omega/(\text{cm}^2 \text{ GHz})$.

The optimization of the end cells incorporates six free parameters per side, allowing asymmetrical designs. A schematic of the geometry is presented in Fig. 1. The optimization was carried out with MATLAB's function `fminsearch` an unconstrained downhill simplex search method. Though the solver implemented does not handle constraints (solvers with constraints were frustrated by the problem's non-analyticity), physical requirements necessitate constraining the system. This was accomplished by severely penalizing search points that violate (1) Non-physical/non-smooth geometries, (2) $E_{pk}/E_{acc} < 2.1$, (3) wall angles $> 87.5^\circ$ measured from the horizontal (no re-entrant designs permitted) and (4) small curvatures near the irises, as very small curvatures are technologically challenging.

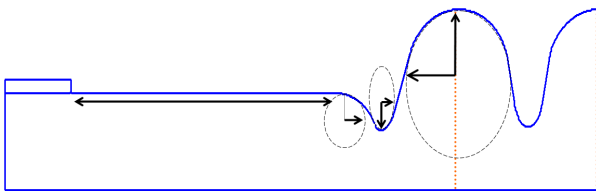


Figure 1: Schematic of the right end cell and first center cell cavity geometry. The figure is to scale and has dimensions very near the optimized geometry. The arrows show the adjustable parameters. The dotted lines mark the repeating center cell structure, whose dimensions remain fixed throughout the optimization. The rectangular structure at the top left is the HOM absorber, which was taken to be TT2.

It is important to note that for each passband, the four combinations of electric and magnetic boundary conditions were solved to simulate a chain of identical cavities. This is more realistic than open boundary conditions because open boundary conditions are only applicable in the case of an isolated cavity, not one in a long chain of cavities. Thus, the HOMs computed here much more accurately reflect what one could expect in the main linac.

The optimization routine minimized the BBU parameters ($=R/Q \cdot Q_L/f$) for higher-order dipole modes from 1.6–5.0 GHz. This is not as simple as simply selecting a single HOM and searching for a geometry minimizing its BBU parameter, which should behave analytically. This is because geometry changes that reduce the strength of one HOM can drastically increase the strength of another HOM. Thus, the problem is to find a cavity shape that simultaneously minimizes the BBU parameters of all the HOMs, is an intrinsically non-analytic process. This is why gradient-search method solvers cannot solve this problem.

07 Cavity design

To simplify the optimization, the simultaneous minimization of n-higher order modes was treated as the analytic problem of minimizing the worst HOM, under the non-analytic constraint that each BBU parameter of all other dipole modes in the spectrum be less than the maximal BBU parameter of all the modes $\equiv M$ [7]. Minimization improves the BBU parameter by controlling the worst mode, all of the other modes are required to fall below M for the point to be in the search space. As the optimization progresses, if all the BBU parameters fall below M , the new worst BBU parameter is assigned to M , otherwise the search point is discarded. This process effectively minimizes all the HOMs simultaneously. Furthermore, should the control HOM be below another mode that had a smaller value earlier in the optimization, the optimization switches to control the new mode. Thus the non-analytic problem is decomposed into an analytic problem with a non-analytic constraint.

The optimization was carried out in parallel on 256 processors leased from Cornell's Center for Advanced computing, and the electro-magnetic fields were solved with 2D finite element codes CLANS for the monopole mode and CLANS2 for dipole modes [4].

After the optimization converged to a solution, the cavity geometry is subjected to small shape perturbations and retuned to regain field flatness of the fundamental mode. Each cell is tuned independently, by keeping the arc length of the cell constant while adjusting the cell length and scaling the r -direction until the fundamental frequency is 1.3 GHz. After tuning, the BBU parameters for all HOMs are computed; a suitable cavity geometry should have BBU parameters that are very similar to the ideal design under small shape perturbations. Optimized cavities were subjected to random deformations uniformly distributed from $\pm 1/16$ mm and $\pm 1/8$ mm, as well as systematic random errors on $\pm 1/8$ mm on all cell parameters

Finally, a subroutine called BMAD [6] was used to simulate an ERL from the properties of the cavities, given a certain frequency spread. BMAD finds the maximum beam current that the design can support. Next, ERLs were constructed from ideal cavities with an "artificial" frequency spread (artificial in the sense that there is no physical origin of this frequency spread, but rather is simply an input parameter to the problem) and lattices constructed of cavities with realistic random cell shape errors and systematic errors (non-identical cavities at the lattice points). Because the cavities with perturbations are different, they are the source of the relative HOM frequency spread, and no artificial spread is introduced. The ERL lattice used for these studies was CERL version 7.4.

RESULTS

Optimizing the end cell design reduced the worst HOM BBU parameter from $20 \times 10^4 \Omega/(\text{cm}^2 \cdot \text{GHz})$ to $8 \times 10^3 \Omega/(\text{cm}^2 \cdot \text{GHz})$ in the range from 1.6–5.0 GHz. Then the design was subjected to realistic shape perturbations, and the

HOMs recomputed. The results of these perturbations are shown in Fig. 2. The BBU parameters for two passbands (2.5 and 3.4 GHz) take on values two to three orders of magnitude greater than design value.

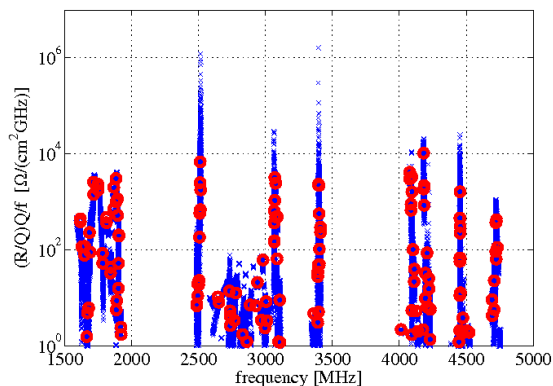


Figure 2: BBU parameter for $\pm 1/16$ perturbations of the baseline design. The HOM BBU parameters are plotted versus frequency. The red circles are the original values of the BBU parameter and the blue crosses are the BBU parameters for 400 perturbed cavities. Note that at 2.5 GHz the worst BBU values are 2 orders of magnitude worse than the design value and at 3.4 GHz, the worst modes are 3 orders of magnitude worse.

Clearly, this first design was very unstable under shape perturbations. To remedy this issue, the width of narrow frequency passbands with strong HOMs were maximized. Table 1 presents the frequency width of the first 6 dipole passbands before and after optimization. The width of the narrowest band was doubled and the second narrowest band was tripled. A comparison of figures of merit and geometry parameters for the original and optimized cells are presented in Table 2.

The end cells were again optimized with this new center cell design, and then the new geometry was again subjected to shape perturbations to study their effect on HOMs. Perturbations were: uniformly distributed random shape variations in the range $\pm 1/16$ mm, uniformly distributed random shape variations of $\pm 1/8$ mm, and random systematic errors of $\pm 1/8$ mm. Each perturbed cavity was tuned as described above prior to HOM calculations. The results of these perturbations are presented in Figs. 3–5.

These results show that optimized cavities using the new center cells allow the design to be stable under perturbations. To finalize the study however, the threshold current produced by these cavities should be explored. One-hundred sample ERLs were generated using the ideal designs and an “artificial” relative frequency spreads of 0, 1.67×10^{-3} , and 3.33×10^{-3} (for both the old and new center cells), and for cavities with random and systematic perturbations. The threshold current computed by BMAD is displayed in Fig. 6.

Figure 6 shows that as the relative frequency spread in-

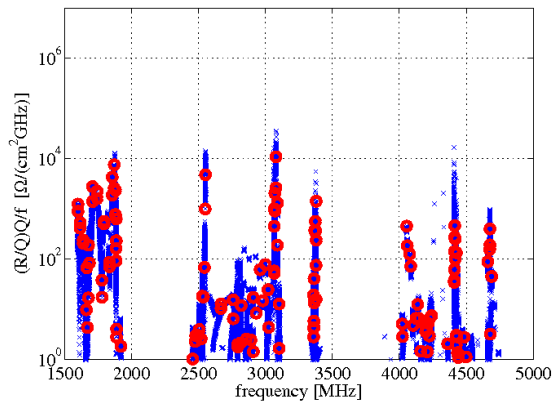


Figure 3: BBU parameter for $\pm 1/16$ shape perturbations of the optimized design with new center cells. The HOM BBU parameters are plotted versus frequency. The red circles are the original values of the BBU parameter and the blue crosses are the BBU parameters for 400 perturbed cavities. Instead of having BBU parameters several orders of magnitude larger than the design value, perturbed cavities are at most a factor of 3 worse than the ideal case for the optimized bands.

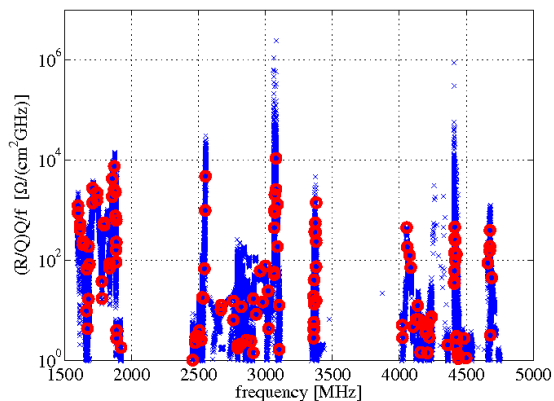


Figure 4: BBU parameter for $\pm 1/8$ shape perturbations of the optimized design with new center cells. The HOM BBU parameters are plotted versus frequency. The red circles are the original values of the BBU parameter and the blue crosses are the BBU parameters for 400 perturbed cavities. The 2.5 GHz passband does not further deteriorate under the larger perturbation, but the 3.1 and 4.4 GHz bands have BBU parameters 2–3 orders of magnitudes worse than design value.

creases, so does the threshold beam current. Note that the “ideal” ERL, constructed from unperturbed cavities, supports higher beam current in the original design, than in the design with re-optimized center and end cells. For ERLs constructed from ‘realistic’ shape perturbed cavities, however, the new design sustains at least 70% more beam current than the old design. Note that the new center cell de-

Table 1: The frequency width of the first 6 dipole passbands [MHz]. Note that bands 3 and 6 were widened significantly while the other bands had their widths decreased only slightly.

Band	1.8 GHz	1.9 GHz	2.5 GHz	2.7 GHz	3.1 GHz	3.4 GHz
Baseline Design	192	95	31	277	55	10
New Design	188	73	107	227	47	20

Table 2: Comparison of figures of merit and geometries for center cells before and after optimization. Cryogenic losses are slightly increased. The geometry factor and E_{pk}/E_{acc} are for the fundamental mode. Key: Eq.=Equator, Horiz.=Horizontal, Vert.=Vertical. The last four dimensions are half-axes of ellipses, measured in cm.

	$R/Q \cdot G$	$\frac{E_{pk}}{E_{acc}}$	Wall Angle	Iris Radius	Eq. Horiz.	Eq. Vert.	Iris Horiz.	Iris Vert.
Baseline	15576 Ω	2.00	85°	3.500	4.399	3.506	1.253	2.095
New Design	14837 Ω	2.06	77°	3.598	4.135	3.557	1.235	2.114

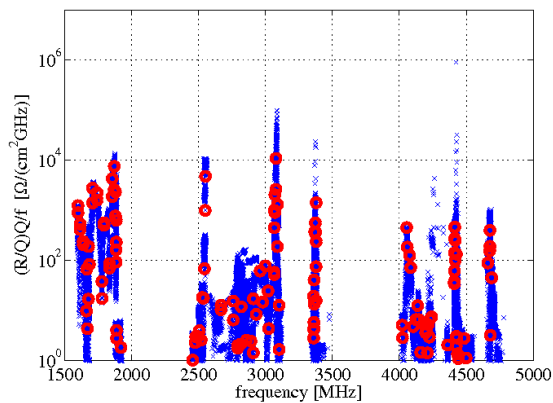


Figure 5: BBU parameter for $\pm 1/8$ systematic shape perturbations of the optimized design with new center cells. The HOM BBU parameters are plotted versus frequency. The red circles are the original values of the BBU parameter and the blue crosses are the BBU parameters for 400 perturbed cavities. Note that the design is much more stable under systematic perturbations than under completely random perturbations, with only one HOM in one cavity having a value of more than $10^5 \Omega/(\text{cm}^2 \cdot \text{GHz})$.

sign with 1/8 mm random shape perturbations performs better than an ERL constructed of cells with 1/16 mm random shape perturbations. This is because even though the BBU parameter increases with increasing machine errors, the frequency spread also increases. The net effect is that the current is higher in the $\pm 1/8$ mm perturbation case. Finally, an ERL constructed of cavities that only have systematic shape errors performs the best of all, with threshold current of over 400 mA.

Continuing the study of higher-order dipole modes, HOM properties up to 10 GHz were also studied. The BBU parameter of the optimized design with new center cells of the 5.1 GHz mode was $5.5 \times 10^6 \Omega/(\text{cm}^2 \cdot \text{GHz})$, or almost 100 times larger than the worst mode below 4.9 GHz. Us-

ing the same optimization procedure as described above, the worst mode has been reduced to $1.6 \times 10^4 \Omega/(\text{cm}^2 \cdot \text{GHz})$ in preliminary optimization. Since, however, this is still a work in progress, there are no perturbation studies nor BMAD simulations available as yet. Examining previous data suggests that for long superconducting RF linacs with hundreds of cavities, the BBU current may not scale as $(R/Q \cdot Q_L/f)^{-1}$ but as $(R/Q \cdot Q_L^c/f)^{-1}$, where $c \approx 1/2$. In this case, the strength of HOMs with high Q_L s may actually be much less important than previously considered, and the optimization already performed would provide sufficient results.

CONCLUSIONS

Optimization of the cavity by decomposing the problem of minimizing all the BBU parameters into minimizing a single mode while keeping all modes below an ever decreasing ceiling is effective in finding a design capable of supporting high threshold currents. Optimizing the end cells alone, however, was not effective in creating a cavity stable under small shape perturbations. To accomplish this, the center cells had to be optimized to strongly couple to one another.

When simulating a realistic ERL with cavities having small shape imperfections from fabrication errors, the case with the new center cells actually maintains a larger average threshold current when subjected to larger shape perturbations (1/8 mm versus 1/16 mm). This is because even though the BBU parameter is increased under larger perturbations—a negative effect—the relative frequency spread is increased—a positive effect—leading to greater average threshold currents. The end result is that simulations show that a realistically designed ERL based on the optimized cavity design is capable of currents ≥ 250 mA.

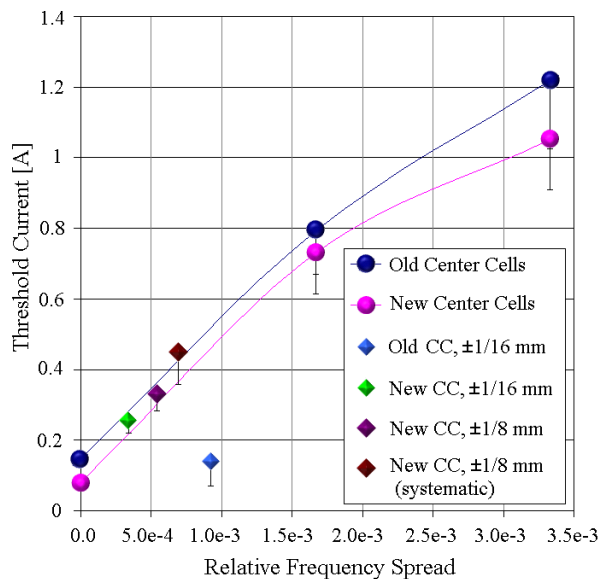


Figure 6: Average beam break-up current versus relative frequency spread for simulated ERLs. The points connected by smoothed lines are ERLs constructed from identical, ideal cavities with artificial frequency spread introduced. The single points are the average threshold current of cavities subjected to simulated machining errors. The error bars mark the minimum threshold current for 90% of the cavities. While an ERL constructed from ideal cells of original cavity design had a larger threshold current than the ideal cells of the new design, an ERL constructed from perturbed cavities was only able to sustain currents of 150 mA, compared to at least 250 mA for shape perturbations of the new design. An ERL with cavities having systematic shape errors of the new design can sustain currents of greater than 400 mA.

REFERENCES

- [1] J. A. Crittenden et. al. "Developments for Cornell's X-Ray ERL," Proceedings PAC09, Vancouver/Canada (2009).
- [2] V. D. Shemelin "Suppression of HOMs in a Multicell Superconducting Cavity for Cornell ERL," Proceedings SRF 2009, Berlin/Germany (2009).
- [3] I. Bazarov, G. Hoffstaetter, Multi-pass Beam Break-Up: Theory and Calculation, EPAC 2004, Lucerne (2004).
- [4] D.G. Myakishev, "CLANS2-A Code for Calculation of Multipole Modes in Axisymmetric Cavities with Absorber Ferrites", Proceedings of the 1999 Particle Accelerator Conference, New York, 1999, pp 2775-2777.
- [5] H. Padamsee, J. Knobloch and T. Hays, "RF Superconductivity for Accelerators," Wiley (1998).
- [6] D. Sagan, "The Bmad Reference Manual," Revision 11.5 (2009). <http://www.lns.cornell.edu/~dcs/bmad/manual.html>
- [7] Personal Communication with J. Sethna and M. Transtrum of Cornell University.